Journal of Environmental Ecology

https://jee.cultechpub.com/jee

E-ISSN: 3093-8074

Vol. 2, No. 2, October 2026

DOI: 10.64229/zkxf5z57

Cultech Publishing

Article

Advancing Micro-Ecotone Mapping Using UAV Photogrammetry and GIS

Bibi Hafsa, Sifatul Hoque Siam*, Mahib Reza, Ripa Akter, Khandakar Hasan Mahmud

Department of Geography and Environment, Jahangirnagar University, Savar, Dhaka-1342, Bangladesh

*Corresponding author: Sifatul Hoque Siam, siam.50@geography-juniv.edu.bd

Abstract

Ecotones are transitional boundaries between ecosystems and essential to regulating biodiversity and ecological processes. Although ecotones are often wider transition zones like aquatic-terrestrial boundaries, they can happen at fine spatial scales (micro-ecotones) and occur over only a few meters or even centimeters. In the past, ecotones have been examined using one-dimensional transects or coarsely resolved remote sensing data for analysis. However, such methods have been too coarse to detect the fine-scale spatial heterogeneity of micro-ecotones. This work develops a geospatial framework to map fine-scale aquatic-terrestrial micro-ecotones at Jahangirnagar University, Bangladesh, utilizing high-resolution unmanned aerial vehicle (UAV) photogrammetry integrated with geographic information systems. High-resolution RGB imagery was obtained using a DJI Mavic Pro and at a height of 200 ft, producing a 3 cm vertical accuracy. Object-based image classification was applied in ArcGIS Pro using support vector machine classifiers, spectral indices, textural measures, and structural features derived from digital elevation model and canopy models to delineate micro-ecotones. The accuracy assessment confirmed that a high degree of accuracy (96.20%, Kappa coefficient- 0.9584) exists between the orthomosaic and classified image. The data analysis revealed a specific spatial pattern in micro-ecotone distribution, with a significant decrease in micro-ecotone density with increasing elevation. In addition, Spearman correlation analyses clearly revealed a strong negative relationship (–0.971) between elevation and micro-ecotone occurrence, confirming that micro-relief features and water proximity are key factors that regulate micro-ecotone occurrence. The combination of UAV imagery, OBIC, and field verification can be used for micro-ecotone configuration and vegetation distribution.

Keywords

Ecotone, Micro-ecotone, Unmanned aerial vehicle photogrammetry, Object-based image classification, Digital elevation model

Article History

Received: 24 April 2026
Revised: 07 September 2026
Accepted: 28 September 2026
Available Online: 13 October 2026

Copyright

© 2026 by the authors. This article is published by the Cultech Publishing Sdn. Bhd. under the terms of the Creative Commons Attribution 4.0 International License (CC BY 4.0): https://creativecommons.org/licenses/by/4.0/

1. Introduction

Ecotones represent boundary regions between different habitats and can occur across a wide range of spatial and temporal scales [1-3]. The concept of the ecotone was first introduced by Clements, who described it as a transition zone where dominant species from adjacent communities reach their distributional limits [4]. Broadly, ecotones have a set of functions, acting as ecological interfaces that regulate energy flow, facilitate species interactions, enhance biodiversity, and often create unique assemblages of flora and fauna [5-7]. Because of their sensitivity to spatial and temporal changes, ecotones have long been considered as crucial in geographical aspects, biodiversity conservation, ecological monitoring, agricultural uses and environmental management [6,8,9].

However, when explored at finer spatial scales, micro-ecotones are realized as small, localized transition zones within a wider landscape [10,11]. Micro-ecotones can occur across distances as small as a few meters, or even centimeters, but have a disproportionate impact upon a regime of ecological processes [10]. Micro-ecotones are particularly evident in heterogeneous landscapes such as grasslands, riparian corridors, and wetland margins, where subtle variations in micro-topography, elevation change, soil moisture, and light availability result in distinct shifts in vegetation composition [12-14].

The aquatic-terrestrial boundary represents a critical zone where micro-ecotones emerge within grassland-dominated landscapes [15]. In these areas, subtle elevation differences and hydrological processes intersect with terrestrial herbaceous vegetation (such as grasses, forbs and scattered shrubs) creating highly dynamic and ecologically significant transition zones [16,17]. These individual boundary regions often support species richness that is comparable yet distinct from that of broader ecotones, reflecting the fine-scale ecological variability of micro-ecotones [18,19].

Ecotone delineation is a central concern in vegetation ecology, as it provides insights into plant community organization and the ecological processes operating between adjacent ecosystems [20]. Earlier studies often relied on edge-detection techniques based on one-dimensional transect method such as moving split window (MSW) [21], Ordination techniques [22], Sigmoid wave curve fitting [23], Wavelets [24]. Among these, the MSW method has been the most widely applied for identifying transition zones [25]. However, one-dimensional approaches have limitations in effectively representing the spatial characteristics of ecotones such as their location, morphology, and patterns of distribution, constraining a complete understanding of boundary dynamics [26]. To compensate for such limitations, two-dimensional boundary detection methods has been invented. These methods have mainly been based on image analytical methods and are employed through rasterized digital information derived from satellite images or photogrammetric products [26,27]. Common methods include clustering techniques [28], fuzzy logic methods [29], wombling methods [30], and spatial statistical analyses [31], all of which present an improved two-dimensional representation of ecotone structures.

Unmanned aerial vehicles (UAVs) have transformed ecological monitoring by providing high-resolution, flexible, and cost-effective data acquisition for landscape-scale studies [32,33]. In ecotone research, UAVs offer distinct advantages over conventional one-dimensional transect or pixel-based remote sensing approaches [34]. High-resolution UAV imagery can quantify subtle variations in vegetation height, canopy structure, and spatial distribution, enabling the delineation of narrow transition zones that are often missed in coarser datasets [35,36]. Studies have demonstrated the use of UAV-derived RGB imagery for estimating tree and crop heights, biomass, and canopy structure, providing a framework for applying similar approaches to ecotone mapping and landscape heterogeneity analysis [37-39]. Integration of UAV data with GIS and object-based image analysis (OBIA) further enhances boundary detection, allowing the identification of ecotone width, shape complexity, and structural diversity [40-43]. This approach allows to assess both the structural and functional aspects of ecotones, monitor ecological responses to environmental change [44]. In the context of micro-ecotones, UAVs enable detection of subtle elevation or hydrology-driven vegetation transitions, offering a robust and scalable method for monitoring small-scale ecological boundaries [45,46].

In this study, we present a comprehensive methodological approach to identify boundaries of aquatic-grassland ecosystems by UAV based image and geographic information system (GIS) data. By integrating spectral, topographic, and structural information extracted from high-resolution UAV images, this approach enables a sophisticated characterization of micro-ecotone processes that are often gradual or subtle in their expression.

2. Materials and Methods

2.1 Study Area

The research site is confined to a particular small area of Jahangirnagar University, located in Savar, 32 kilometers northwest of Dhaka, Bangladesh. The absolute location of Jahangirnagar University is between 23.867°-23.898°N and 90.259°-90.273°E. The campus of Jahangirnagar University, which spans 697.56 acres, is characterized by a slightly undulating landscape featuring red lateritic soils, forested areas, and extensive wetlands [47]. Within this context, the area of interest is identified as a transition zone that bridges terrestrial and aquatic ecosystems, predominantly exhibiting grassland vegetation. The presence of both permanent and seasonal wetlands significantly impacts soil moisture

conditions and vegetation composition, rendering this grassland boundary an ecologically important location for detailed ecotone investigation (Figure 1).

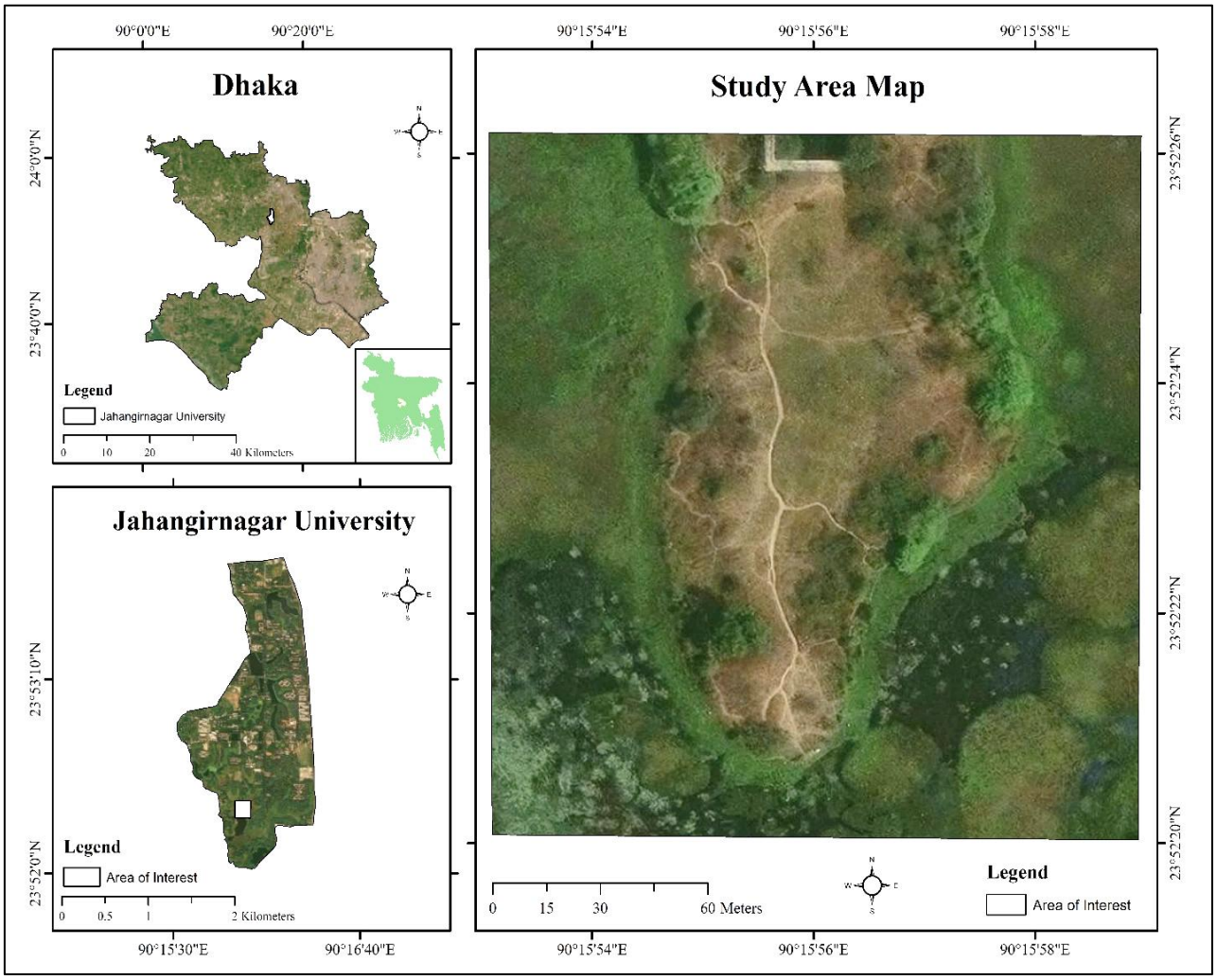

Figure 1. Study area map showing the terrestrial–aquatic transition zone in Jahangirnagar University.
Source: Completed by the authors (2026).

2.2 Data and Methodology

This research utilized primary and secondary sources of data. Primary data were collected from field surveys, direct field observations, and photographic records, while secondary data were sourced from published books, and peer-reviewed journals. These sources provided background knowledge for the study. To identify micro-ecotones and assess spatial patterns, a number of tools were utilized, including ArcGIS Pro for spatial analysis, Plantify for vegetative identification, and DroneDeploy and Pix4D for UAV photogrammetric processing. The overall methodological framework employed in this study is given in Figure 2 below:

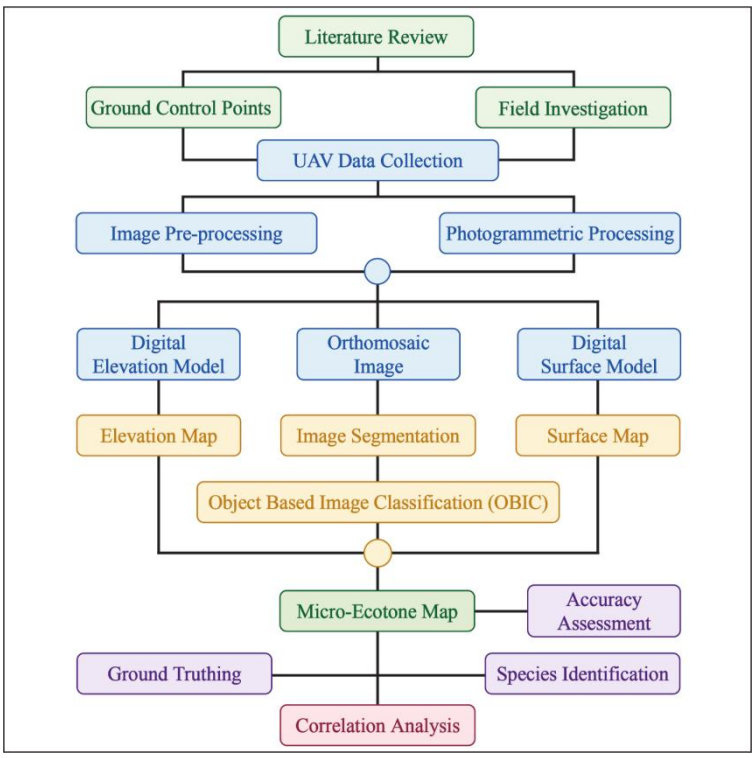

Figure 2. Methodological framework.
Source: Completed by the authors (2026).

2.2.1 UAV Image Data Collection and Processing

High-resolution UAV imagery was acquired to detect the micro ecotones based on photogrammetric technique. The DJI Mavic Pro (UAV) equipped with a 12 MP CMOS sensor (focal length 26 mm equivalent) has been used which captures high-resolution red [R], green [G], and blue [B] images for aerial photography. The ground sampling distance (GSD) defines the spatial resolution of UAV images. It can be calculated using an equation.

$$GSD = \frac{H \times S}{f \times I}$$

Where,
H = Flight height (m)
S = Sensor size (mm)
f = Focal distance (mm)
I = Dimension of the image (pixels)

DJI Mavic Pro is capable of collecting images at a GSD of ≈2.0 cm/pixel at the selected flight height of 200 ft (≈61 m). The platform has used an intelligent flight control system, a pre-programmed flight plan was designed in DroneDeploy (v.4.9, Android platform) to ensure systematic coverage of the study area. The flight plan was executed with 80% forward overlap and 60% side overlap to cover the terrestrial-aquatic transition zone. For ensuring positional accuracy, five ground control points (GCPs) were established. These GCPs were set throughout the study site using a handheld differential GPS with the horizontal accuracy of ± 2 cm. These GCPs were visually marked and integrated during the processing stage for georeferencing and geometric correction of the imagery. Post-flight processing was performed in Pix4D Mapper (v.4.7) following a structure-from-motion (SfM) workflow, including key point extraction and matching, generation of a sparse and dense point cloud (≈12 million points), and classification into terrain and non-terrain features. As output products, a georeferenced orthomosaic with a spatial resolution of 3 cm and a digital surface model (DSM) with a vertical accuracy of ±4 cm was generated. Inclusion of GCPs ensured high spatial fidelity such that ecotone boundaries could be successfully detected as well as mapped.

In order to acquire complete and consistent remote sensing data, this study undertakes the following major steps: (1) Image acquisition was performed on a cloudless sunny day for a minimum number of shadows; (2) A regular UAV flight planning was prepared that ensured constant altitude, overlap, and coverage for the entire area under investigation; (3) GCPs were laid out and measured with differential GPS for enhanced georeferencing quality. (4) High-resolution images were processed through photogrammetric workflows by Agisoft Metashape Professional (64 bit) to generate orthomosaic, digital elevation model (DEM) and DSM.

2.2.2 Generation of DEM and DSM

High-resolution DSM and DEM datasets were created from the UAV imagery based on the SfM technique of

photogrammetry. These processes entailed the steps of alignment, camera calibration, estimation of camera positions and orientations, sparse point cloud creation, dense point cloud creation, and surface modeling. The overlapping images taken by UAVs facilitated three-dimensional modeling of the study area through multi-view image matching. The generated dense point cloud formed the distribution of the surface features in three dimensions which included terrain, vegetation, structures, and any other objects above ground. The point cloud was then interpolated into an extremely high-resolution DSM which depicted the elevation of all the visible surface features. The ground points were then distinguished from the non-ground objects by means of point cloud classification and filtering. The relationship between the two elevation models can be conceptually illustrated as follows: DSM = Ground Surface + Above-Ground Features. Accordingly, the relative height of surface objects can be estimated as: Object Height = DSM – DEM. The elevation map and surface height map were created using a high-resolution DEM data that was derived from UAV photogrammetry results.

2.3 Segmentation and Micro-Ecotone Extraction

In order to define the micro-ecotones, an object-based image classification (OBIC) method was applied in ArcGIS Pro. It was similarly illustrated by [48] for the extraction of green areas for providing methodological basis for the current study. The orthomosaic was imported as the first step within the ArcGIS Pro environment, followed by the application of the Segmentation tool in the Image Classification module for conducting the segmentation. High spectral details (18.5) as well as high spatial details (19) were optimized for the generation of fine objects at the suitable scale for ecotone mapping. A preview of the segmented image was checked for the proper definition of landscape features before the classification. Following this, from the Image Classification Wizard tool, supervised classification method and object-based classification type was used. Following the process of segmentation, a training sample manager was used to develop 200 randomly scattered training samples within the study area. Classification utilized an SVM (Support Vector Machine) algorithm, supporting up to 300 samples per category. Chromaticity color and mean digital number were determined as the main attributes of objects for entering the classifier. The initial classification culminated in the development of three main land-cover classes: vegetation, non-vegetation and water.

Since the main focus of this study was on vegetation-based ecotone dynamics, later analyses were not conducted on non-vegetation classes like open water and aquatic vegetation. For this principal component analysis method was used [49]. The vegetation class was then classified on an additional level as core transition (micro-ecotone) areas. Enhancements covered (i) spectral indices, (ii) textural statistics derived from the gray-level co-occurrence matrix, contrast and dissimilarity, and (iii) structural features extracted using the DEM and the DSM. Vegetation objects having similar spectral as well as structural features were categorized as micro-ecotones representing particular surface in aquatic-terrestrial transition zone.

The applied OBIC reclassification workflow enabled accurate extraction of micro-ecotones through systematic omission of non-vegetation areas unrelated to the identification task as well as augmentation of the vegetation subclasses, thereby ensuring the resulting boundary depicted ecologically relevant transitions in the aquatic-terrestrial mosaic.

2.3.1 Accuracy Assessment

The accuracy assessment of micro-ecotones was designed as follows: geo-statistical sampling in order to generate random points over the map, ground-truthing for assessing validity, formulating a confusion matrix in order to determine producer accuracy (PA), user accuracy (UA), overall accuracy (OA) and finally Kappa coefficient at pre-assumed 95% confidence level. For accuracy assessment at pre-assumed confidence level the following formula has been used.

$$n = \frac{Z^2 pq}{E^2}$$

Where,
n = required sample size
Z = Z score for the chosen confidence level
p = expected accuracy
$q = 1 - p$
E = allowable error

The OA was calculated as the ratio of correctly classified reference points to the total number of reference points and was expressed as a percentage:

$$\text{Overall Accuracy} = \frac{Number\ of\ classified\ points}{Total\ reference\ points} \times 100$$

Producer's accuracy represents the probability that a reference feature was correctly classified and was calculated as:

$$\text{Producer's accuracy} = \frac{Correctly\ classified\ points\ of\ a\ class}{Total\ reference\ points\ of\ that\ class} \times 100$$

To further evaluate the agreement between the classified and reference datasets while accounting for agreement that may occur by chance, the Kappa coefficient (kappa) was calculated:

$$\text{Kappa coefficient} = \frac{P_0 - P_e}{1 - P_e}$$

Where,
P_0 = observed agreement
P_e = agreement expected by chance

The observed agreement was calculated as:

$$P_0 = \frac{\sum_{i=1}^{k} x_{ii}}{N^2}$$

P_0 = observed agreement
x_{ii} = correctly classified samples for class i
N = total number of reference samples

The expected agreement was calculated as:

$$P_e = \frac{\sum_{i=1}^{k} (R_i C_i)}{N^2}$$

P_e = expected agreement by chance
R_i = Rinumber of reference samples for class i
N = total number of reference samples

These accuracy measures provided quantitative evidence of the reliability of the UAV-based micro-ecotone classification.

2.3.2 Ground Validation and Species Identification

In order to prove the results of the UAV-based ecotone mapping, a field survey was carried out following the quadrat sampling technique. This method was introduced by Charles Flahault and C. Schröter in the late 19th century and was later developed and standardized by Frederic E. Clements and Victor E. Shelford in a book named bio-ecology at 1939 for quantitative vegetation studies [50]. The quadrat method allows for systematic sampling of vegetation composition and structure across ecologically diverse zones.

In this study, a total of 22 quadrats were established across the transition zone to identify species. Particularly, two quadrats were used in a micro-ecotone identified through UAV-based classification. Each quadrat measured 1 m × 1 m, ensuring adequate representation of both dominant and subordinate vegetation layers. Species identification was carried out using plantify application, field guides and verified through standard floristic references.

2.4 Correlation Analysis

To determine the relationship between elevation and the distribution of micro-ecotones, Spearman's rank correlation coefficient (ρ) was employed. Elevation values were extracted from the high-resolution DEM, while the number of micro-ecotones corresponding to each elevation point was obtained from the UAV-based classification results. Spearman's correlation was selected because the variables may not follow a normal distribution and the relationship between elevation and micro-ecotone abundance may not necessarily be linear. This non-parametric method evaluates the strength and direction of a monotonic relationship between two variables based on their ranked values. Spearman's rank correlation coefficient was calculated using the following equation:

$$\rho = 1 - \frac{6\sum_{i=1}^{n} d_i^2}{n(n^2 - 1)}$$

ρ = Spearman's rank correlation coefficient
d_i = Difference between the elevation and micro-ecotone number
n = total number of observations

The value of (rho) ranges from –1 to +1. A positive value indicates that the number of micro-ecotones tends to increase with increasing elevation, whereas a negative value indicates an inverse relationship. A value close to zero indicates a weak or negligible monotonic association.

3. Results and Discussion

3.1 High-Resolution Orthomosaic and DEM-DSM Generation

The UAV photogrammetric workflow resulted in a high-resolution orthomosaic, DEM and DSM that provided the spatial basis for ecotone boundary detection and analysis. The orthomosaic was mapped to the GSD of 3 cm/pixel, which allowed for a fine-scale description of patterns of vegetation and micro-ecotone boundaries in the aquatic-terrestrial transition zone. The integration of five GCPs measured using differentially corrected GPS, provided georeferencing accuracy of ±3 cm and limited geometric distortions which enhanced spatial fidelity of ecotone boundaries.

Visual interpretation of the orthomosaic revealed distinct ecological patterns. Greener vegetation zones were concentrated along the margins of permanent waterbodies, where higher soil moisture supports dense growth of grasses, shrubs, and hydrophytic species. In contrast, upland areas further away from the water appeared drier and less vegetated. The high-resolution orthomosaic showing detailed vegetation patterns, including grasslands and shrubs, along with permanent and seasonal waterbodies is given in the Figure 3.

Figure 3. High-resolution orthomosaic generated from UAV photogrammetry.
Source: Completed by the authors (2026).

The high-resolution DEM and DSM were derived from a dense UAV point cloud (~12 million points), providing both elevation and surface structure information with a vertical accuracy of ±3 cm. Elevation values ranged from 5 m in low-lying wetland depressions to 18 m in higher terrestrial grassland patches, while surface heights captured by the DSM varied from near 0 m in marsh areas to 3-4 m in tall grass and shrub patches. These topographic and structural gradients provided critical context for ecotone mapping: the lowest elevations (5-8 m) and minimal surface heights corresponded to marsh-dominated vegetation, whereas higher elevations (15-18 m) and taller vegetation heights supported dry grassland. Images of high-resolution DEM and DSM are given in Figure 4 below:

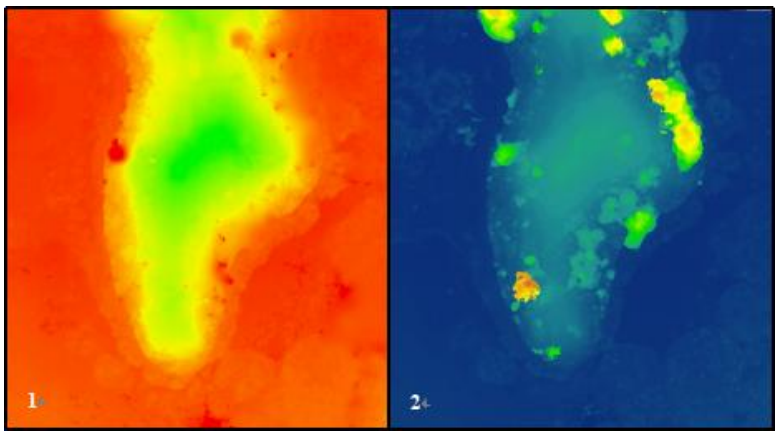

Figure 4. High-resolution DEM and DSM images of the study area. (1) DEM showing elevation gradients (2) DSM showing surface heights.
Source: Completed by the authors (2026).

3.2 Micro-Ecotone Mapping

The micro ecotone distribution map derived from the OBIC workflow reveals a patchy distribution of micro-ecotones, with eleven different types of micro-ecotones mapped in the aquatic–terrestrial transitional area of the study site. The ecotones are centered on subtle elevation changes (5-18 m), indicating that micro-topographic and hydrologic conditions directly influence the distribution of vegetation. Mapped areas with more gradual elevation change exhibited wider transition zones, while areas with steeper topographic changes exhibited sharper boundaries, consistent with previous research citing topography and soil moisture play in determining the extent of ecotones. The UAV-derived classification thus proved effective in capturing subtle species turnover patterns that are typically overlooked in coarser satellite datasets. Spatial distribution map of micro-ecotone is given in the Figure 5 below:

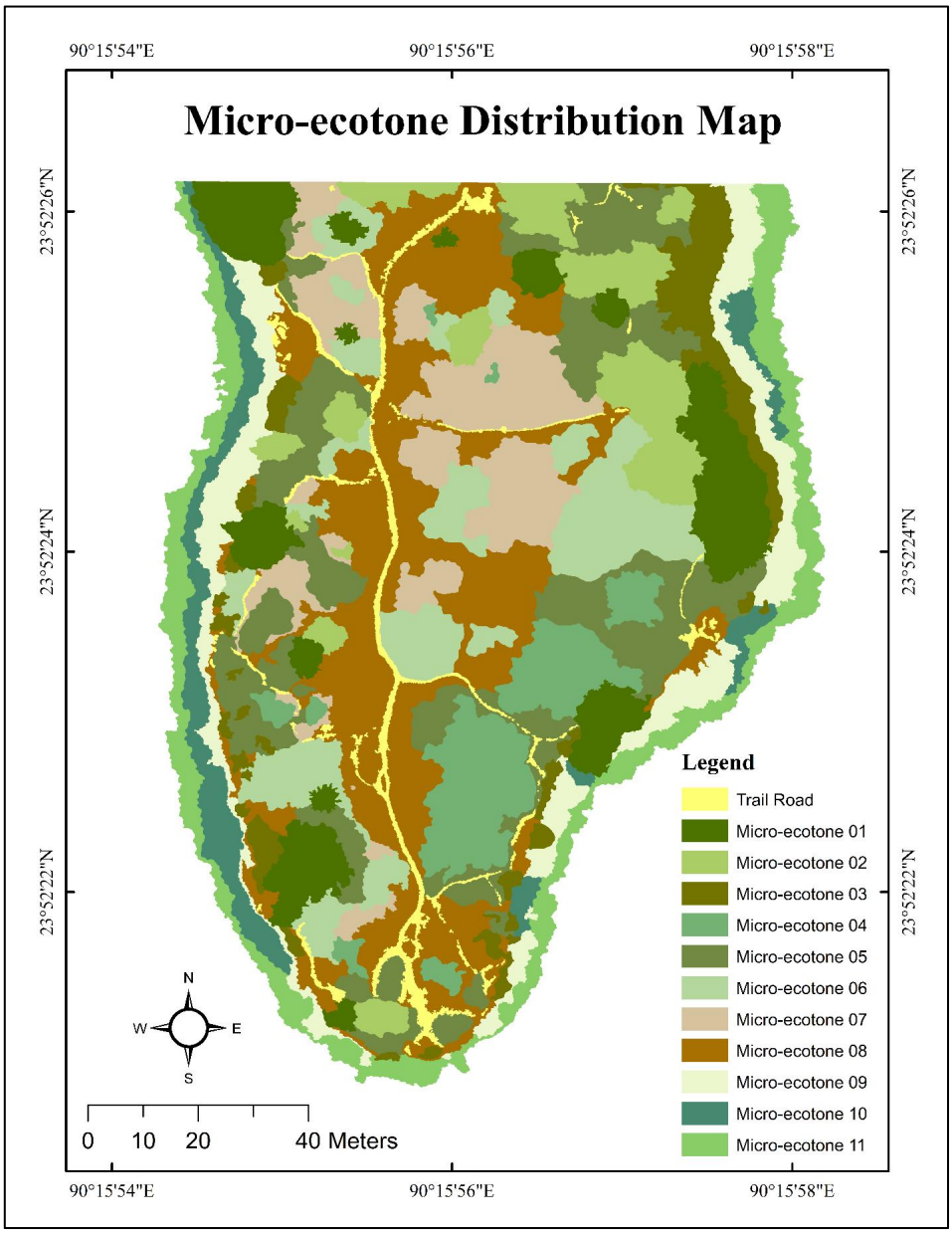

Figure 5. Micro-ecotone distribution map of the study area.
Source: Completed by the authors (2026).

Lower elevations and areas near permanent wetlands showed a higher density of micro-ecotones, whereas upland with fewer transitional zones.

3.3 Accuracy Assessment

The accuracy of the UAV-based object-oriented classification was assessed using an error matrix (confusion matrix) based on independently collected reference points. A calculated total of 316 reference points were used to evaluate the classification performance of the identified classes at 95% pre-assumed confidence level, including the trail road and 11 micro-ecotone classes. The confusion matrix has been given in Table 1.

Table 1. The confusion matrix.

Classified	Trail Road	Ecotone 1	Ecotone 2	Ecotone 3	Ecotone 4	Ecotone 5	Ecotone 6	Ecotone 7	Ecotone 8	Ecotone 9	Ecotone 10	Ecotone 11	Total Reference Point
Trail Road	**14**	0	0	0	0	0	0	0	1	0	0	0	15
Ecotone 1	0	**25**	1	0	0	0	0	0	0	0	0	0	26
Ecotone 2	0	1	**28**	0	0	0	0	0	0	0	0	0	29
Ecotone 3	0	0	0	**21**	0	0	0	0	0	0	0	0	21
Ecotone 4	0	0	0	1	**30**	1	0	0	0	0	0	0	32
Ecotone 5	0	0	0	0	0	**24**	0	0	0	0	0	0	24
Ecotone 6	0	0	0	0	0	0	**26**	1	0	0	0	0	27
Ecotone 7	0	0	0	0	0	0	0	**20**	1	0	0	0	21
Ecotone 8	1	0	0	0	0	0	0	0	**41**	0	0	0	42
Ecotone 9	0	0	0	0	0	0	0	0	0	**27**	1	0	28
Ecotone 10	0	0	0	0	0	0	0	0	0	1	**22**	1	24
Ecotone 11	0	0	0	0	0	0	0	0	0	0	1	**26**	27
Total Classified Points	15	26	29	22	30	25	26	21	43	28	24	27	**316**

Source: Completed by the authors (2026).

The confusion matrix shows that most classes were accurately distinguished, with only a small number of misclassified reference points. Percentages of user's accuracy and producer's accuracy are shown in Table 2. he highest classification performance was observed for Ecotone 3 and Ecotone 5, which achieved 100% user's accuracy, while Ecotone 4 and Ecotone 6 recorded 100% producer's accuracy. These results indicate that these classes were particularly well separated from the other micro-ecotone classes based on their spectral and spatial characteristics. In contrast, Ecotone 10 showed the lowest user's and producer's accuracy, both at 91.67%, although this still represents a high level of classification reliability.

Table 2. Class-wise user's and producer's accuracy of the UAV-based object-oriented classification.

Class	Trail Road	Ecotone 1	Ecotone 2	Ecotone 3	Ecotone 4	Ecotone 5	Ecotone 6	Ecotone 7	Ecotone 8	Ecotone 9	Ecotone 10	Ecotone 11	Mean
User's Accuracy[%]	93.3	96.15	96.5	100	93.75	100	96.3	95.24	97.62	96.43	91.67	96.3	96.11
Producer's Accuracy [%]	93.3	96.15	96.5	95.4	100	96	100	95.24	95.35	96.43	91.67	96.3	96.04

Source: Completed by the authors (2026).

The user's accuracy ranged from 91.67% to 100%, with a mean of 96.11%, indicating a low probability of commission error across the classified classes. Similarly, producer's accuracy ranged from 91.67% to 100%, with a mean of 96.04%, demonstrating a low omission error. The Trail Road class achieved 93.33% for both user's and producer's accuracy. Most of the remaining ecotone classes recorded accuracies above 95%, demonstrating consistent classification performance across the study area. Most of the remaining ecotone classes recorded accuracies above 95%, demonstrating consistent classification performance across the study area. The assessment produced an OA of 96.20% and a Kappa coefficient of 0.9584, indicating almost perfect agreement between the UAV-based classification and the reference data.

3.4 Ground Truthing and Dominant Species Identification

Ground truthing was conducted using quadrat method to validate the accuracy and ecological relevance of the UAV-derived ecotone classification. A total of 22 quadrats were established systematically across the mapped transition zones. Each quadrat measured 1 m × 1 m and was positioned to include the core vegetation of the transition areas. Within each quadrat, dominant species were identified. Table 3 gives the ecotones and their dominant species with their scientific names below:

Table 3. Identified dominant species across different ecotones.

Micro-ecotone	Dominant Species (Common Name)	Scientific Name
Micro-ecotone 01	Southern cutgrass	*Leersia hexandra Sw.*
Micro-ecotone 02	Clove basil	*Ocimum gratissimum*
Micro-ecotone 03	Large-Leaf Smilax	*Smilax ovalifolia Roxb.*
Micro-ecotone 04	Cutleaf groundcherry	*Physalis 10ngulate L.*
Micro-ecotone 05	False buttonweed	*Spermacoce articularis L.*
Micro-ecotone 06	Cinderella Weed	*Synedrella nodiflora*
Micro-ecotone 07	Caesarweed	*Urena lobata*
Micro-ecotone 08	Kans grass	*Saccharum spontaneum*
Micro-ecotone 09	Dwarf Morning Glory	*Evolvulus nummularius*
Micro-ecotone 10	Torpedograss	*Panicum repens*
Micro-ecotone 11	Alligator weed	*Alternanthera philoxeroides*

Source: Completed by the authors (2026).

Field-based species identification revealed a clear correspondence between UAV-derived micro-ecotone classes and observed vegetation composition. Eleven distinct micro-ecotones were confirmed through dominant species presence (Table 3), indicating strong agreement between remote sensing outputs and ground observations. The distinct dominance of different plant species across micro-ecotones provides strong ecological evidence supporting the validity of the UAV-based classification. The close agreement between field observations and mapped micro-ecotones demonstrates that high-resolution UAV imagery combined with object-based classification techniques is effective in detecting subtle vegetation boundaries. These results highlight the ecological significance of micro-ecotones as zones of rapid species turnover and reinforce their role as sensitive indicators of environmental gradients in aquatic–terrestrial transition zones.

3.5 Correlation Analysis

The research examined the relationship between elevation and the amount of total micro-ecotones through elevation data collected from UAV and confirmed in the field survey. The data indicates an inverse relationship between elevation and the amount of micro-ecotones (Table 4, Figure 6).

Table 4. Relationship between elevation and micro-ecotone numbers.

Contour	Total Micro-ecotone
18	3
16	4
12	4
9	6
8	6
5	8

Source: Completed by the authors (2026).

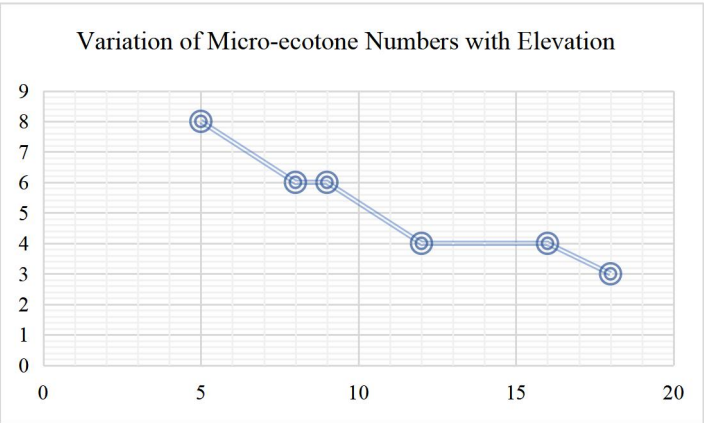

Figure 6. Variation of micro-ecotone numbers with elevation.
Source: Completed by the authors (2026).

The lower elevation, particularly elevation of 5 m, contained the highest number of micro-ecotones (8). The higher elevation contained fewer micro-ecotones, with only 3 micro-ecotones observed at 18 m. The mid-range elevation decreased steadily, with 6 in the range of elevation 8-9 m and 4 for elevation in the range of 12-16 m.

Based on Spearman's rank correlation coefficients, there is a strong, inverse correlation between elevation and density of micro-ecotones (R = –0.971) at the 0.01 level (p = 0.001). This finding confirms that the relationship continues to be associated together in a consistent way, even when assessing the relationship as a monotonic trend as opposed to strictly linear (Table 5).

Table 5. Result of Spearman's rank correlation coefficients.

		Elevation	**Number of Micro-ecotones**
Elevation	Correlation Coefficient	1.000	–0.971*
	Sig. (2-tailed)	–	0.001
	N	6	6
Number of Micro-ecotones	Correlation Coefficient	–0.971*	1.000
	Sig. (2-tailed)	0.001	–
	N	6	6

* Correlation is significant at the 0.01 level (2-tailed).
Source: Completed by the authors (2026).

4. Discussion

The findings demonstrate that micro-ecotone distribution within the aquatic–terrestrial transition zone is strongly controlled by fine-scale topographic and hydrological conditions. The UAV-derived orthomosaic, DEM, and DSM provided sufficient spatial detail to identify subtle vegetation transitions and micro-ecotone boundaries that are difficult to represent using conventional coarse-resolution remote sensing data. The mapped micro-ecotones showed a clear concentration at lower elevations, particularly around 5-9 m, whereas their occurrence decreased toward the higher elevations of 12-18 m. This pattern is supported by the strong negative Spearman's rank correlation between elevation and micro-ecotone number ($r_s = –0.971$, $p = 0.001$), indicating that micro-ecotone occurrence decreases systematically with increasing elevation. Lower-lying areas are more closely associated with wetlands and waterbodies and therefore experience greater hydrological influence, soil-moisture availability, and vegetation transitions, whereas higher areas are relatively less influenced by aquatic conditions and support more homogeneous terrestrial vegetation. The spatial distribution also showed greater micro-ecotone density near permanent waterbodies, suggesting that hydrological proximity contributes substantially to the formation and maintenance of fine-scale ecological transition zones. The high classification accuracy (96.20%) and Kappa coefficient (0.9584) further demonstrate the reliability of the UAV-based object-oriented classification for delineating these fine-scale features. Overall, the findings indicate that micro-topographic variation and hydrological influence jointly regulate micro-ecotone formation, while the integration of UAV photogrammetry, object-based image classification, DEM/DSM analysis, and field observations provides an effective framework for characterizing fine-scale aquatic–terrestrial ecological transitions.

5. Conclusion

This study proves the effectiveness of combining high-resolution UAV photogrammetry with object-based image classification and analysis of fine-scale aquatic-terrestrial micro-ecotones. The approach utilized centimeter accuracy orthomosaic imagery with DEM and DSM derived topography as well as field supervised vegetation composition. As it can be noted, the proposed approach effectively mapped fine-scale ecological transitions that usually remain undetected with the aid of traditional transect analyses or coarse-scale remotely sensed datasets. The methodology proves that micro-ecotones occur as organized landscape features depending mostly on topography at the micro-scale and hydrological proximity.

Future studies may improve this approach by adding multi-temporal UAV data to study the seasonal or inter-annual variation of micro-ecotones, and multispectral/hyperspectral images for enhanced species-level identification. Replication of the approach with varying landscape types will also help to generalize it for applications pertaining to landscape, wetland, and climate change impact assessments.

Acknowledgements

The authors acknowledge the Spatial Analysis Lab, Jahangirnagar University, Savar, Dhaka 1342, Bangladesh for providing UAV for this research.

Funding

This research received no specific grant from any funding agency in the public, commercial, or not for profit sectors.

Ethics Statement

This research does not incorporate any human participation or animal experiments, rather based on remote sensing operations. During fieldwork activities, proper handling of organic environment and biotic life was ensured with high sensitivity and sophistication. Data analysis and management were performed under sincere guidance.

Data Availability Statement

Incorporated datasets are available from the corresponding author upon considerable request.

Author Contributions

Bibi Hafsa: Conceptualization, Research Design, Literature Review, Methodology. Sifatul Hoque Siam: Data Collection, Field Survey Design, Drone Operation, Data Compilation, Data Analysis, Manuscript Drafting & Formatting, Data Visualization. Mahib Reza: Data Collection, Field Survey Design, Drone Survey Design & Operation, Geostatistical Analysis, Manuscript Reviewing, Data Visualization. Ripa Akter: Manuscript Formatting, Review, Data Analysis. Khandakar Hasan Mahmud: Conceptualization, Research Design, Literature Review, Methodology.

Conflict of Interest

The authors declare no conflict of interest.

Generative AI Statement

The authors declare that no Gen AI was used in the creation of this manuscript.

References

[1] Delcourt PA, Delcourt HR. Ecotone dynamics in space and time. In: Landscape boundaries: Consequences for biotic diversity and ecological flows. New York, NY: Springer New York, 1992, 19-54. DOI: 10.1007/978-1-4612-2804-2_2

[2] Rusek J. Distribution and dynamics of soil organisms across ecotones. In: Landscape boundaries: Consequences for biotic diversity and ecological flows. New York, NY: Springer New York, 1992, 196-214. DOI: 10.1007/978-1-4612-2804-2_9

[3] Fortin M J, Olson R J, Ferson S, Iverson L, Hunsaker C, Edwards G, et al. Issues related to the detection of boundaries. Landscape Ecology, 2000, 15(5), 453-466. DOI: 10.1023/A:1008194205292

[4] Clements FE. Research methods in ecology. University Publishing Company. Lincoln, Nebraska, 1905. Available from: https://archive.org/details/researchmethodsi00clemuoft (accessed on 15 July 2025).

[5] Holland MM, Risser PG, Naiman RJ, editors. Ecotones: The role of landscape boundaries in the management and restoration of changing environments. Boston, MA: Springer US, 1991. DOI: 10.1007/978-1-4615-9686-8

[6] Hufkens K, Scheunders P, Ceulemans R. Ecotones in vegetation ecology: Methodologies and definitions revisited. Ecological Research, 2009, 24(5), 977-986. DOI: 10.1007/s11284-009-0584-7

[7] Walker S, Wilson JB, Steel JB, Rapson GL, Smith B, King WM, et al. Properties of ecotones: Evidence from five ecotones objectively determined from a coastal vegetation gradient. Journal of Vegetation Science, 2003, 14(4), 579-590. DOI: 10.1111/j.1654-1103.2003.tb02185.x

[8] Farina A. Scaling Patterns and Processes Across Landscapes. Principles and methods in landscape ecology: An agenda for the second millennium. Cham: Springer International Publishing, 2022, 157-176. DOI: 10.1007/978-3-030-96611-9_4

[9] Kark S. Effects of ecotones on biodiversity. In: Reference Module in Life Sciences. Elsevier, 2017. DOI: 10.1016/B978-0-12-809633-8.02290-1

[10] McArthur ED, Ostler WK, Wambolt CL. Proceedings: Shrubland ecotones. Proc RMRS-P-11. Ogden, UT: US Department of Agriculture, Forest Service, Rocky Mountain Research Station. 1999, 11, 299.

[11] Yando ES, Osland MJ, Hester MW. Microspatial ecotone dynamics at a shifting range limit: Plant–soil variation across salt marsh–mangrove interfaces. Oecologia. 2018, 187(1), 319-331. DOI: 10.1007/s00442-018-4098-2

[12] Corenblit D, Steiger J, Gurnell AM, Tabacchi E, Roques L. Control of sediment dynamics by vegetation as a key function driving biogeomorphic succession within fluvial corridors. Earth Surface Processes and Landforms: The Journal of the British Geomorphological Research Group, 2009, 34(13), 1790-1810. DOI: 10.1002/esp.1876

[13] Antvogel H, Bonn A. Environmental parameters and microspatial distribution of insects: A case study of carabids in an alluvial forest. Ecography, 2001, 24(4), 470-482. DOI: 10.1111/j.1600-0587.2001.tb00482.x

[14] Treble NA. The relationship between vegetation, micro-topography and edaphic factors in a lowland floodplain grassland system, South East England. Brighton: University of Brighton, 2010.

[15] Zheng P, Li C, Ye C, Wang H, Wei W, Zheng Y, et al. Factors driving wetland herbs distribution range of lake-terrestrial ecotone in Tibet, China. 2021. DOI: 10.21203/rs.3.rs-1078363/v1

[16] Johnston CA, Naiman RJ. Boundary dynamics at the aquatic-terrestrial interface: The influence of beaver and geomorphology. Landscape Ecology, 1987, 1(1), 47-57. DOI: 10.1007/BF02275265
[17] Li L, Chen J, Han X, Zhang W, Shao C. Grassland ecosystems of China. Vol. 2. Singapore: Springer Singapore; 2020. DOI: 10.1007/978-981-15-3421-8
[18] Bukhary A, Ruslan MY, Fauzi M, Noorhisham H, Fahmi M, Nicholas S, et al. Micro-habitats' utilization, feeding niche overlapping, and plantation management systems: Impacts on the hymenopteran community tolerances within oil palm plantations. Journal of Advances In Agriculture, 2016, 6(1), 888-904. DOI: 10.24297/jaa.v6i1.5395
[19] Sorokina HE, Campos M, Raumonen P, Shcherbacheva A, Echriti R, Hyyppä J, et al. Boundary conditions for studying branch-scale tree growth strategies using tree quantitative structure model time series. Remote Sensing of Environment, 2026, 333, 115105. DOI: 10.1016/j.rse.2025.115105
[20] Erdős L, Gallé R, Bátori Z, Papp M, Körmöczi L. Properties of shrubforest edges: A case study from South Hungary. Central European Journal of Biology, 2011, 6(4), 639-658. DOI: 10.2478/s11535-011-0041-9
[21] Whittaker. Gradient analysis of vegetation. 42nd ed. Biological Reviews, 1967, 207-257. Available from: https://www.cabidigitallibrary.org/doi/full/10.5555/19670600350 (accessed on 12 June 2025).
[22] Choesin D, Boerner REJ. Vegetation boundary detection: A comparison of two approaches applied to field data. Plant Ecology, 2002, 158(1), 85-96. DOI: 10.1023/A:1014720508155
[23] Timoney KP, La Roi GH, Dale MRT. Subarctic forest-tundra vegetation gradients: The sigmoid wave hypothesis. Journal of Vegetation Science, 1993, 4(3), 387-394. DOI: 10.2307/3235597
[24] Camarero JJ, Gutiérrez E, Fortin M. Spatial patterns of plant richness across treeline ecotones in the Pyrenees reveal different locations for richness and tree cover boundaries. Global Ecology and Biogeography, 2006, 15(2), 182-191. DOI: 10.1111/j.1466-822X.2006.00211.x
[25] Hufkens K, Scheunders P, Ceulemans R. Ecotones in vegetation ecology: Methodologies and definitions revisited. Ecological Research, 2009, 24(5), 977-986. DOI: 10.1007/s11284-009-0584-7
[26] Wang B, Sun H, Cracknell AP, Deng Y, Li Q, Lin L, et al. Detection and quantification of forest-agriculture ecotones caused by returning farmland to forest program using unmanned aircraft imagery. Diversity, 2022, 14(5), 406. DOI:10.3390/d14050406
[27] Rakotoarivony MNA, Gholizadeh H, Hassani K, Zhai L, Rossi C. Mapping the spatial distribution of species using airborne and spaceborne imaging spectroscopy: A case study of invasive plants. Remote Sensing of Environment, 2025, 318, 114583. DOI: 10.1016/j.rse.2024.114583
[28] McIntire EJB, Fortin M-J. Structure and function of wildfire and mountain pine beetle forest boundaries. Ecography. 2006, 29(3), 309-318. DOI: 10.1111/j.2006.0906-7590.04278.x
[29] Brown WM, Groves DI, Gedeon TD. An artificial neural network method for mineral prospectivity mapping: A comparison with fuzzy logic and bayesian probability methods. In: Geophysical applications of artificial neural networks and fuzzy logic. Dordrecht: Springer Netherlands, 2003. 179-196. DOI: 10.1007/978-94-017-0271-3_12
[30] Womble WH. Differential systematics. Science, 1951, 114(2961), 315-322. DOI: 10.1126/science.114.2961.315
[31] Pélissier R, Goreaud F. A practical approach to the study of spatial structure in simple cases of heterogeneous vegetation. Journal of Vegetation Science, 2001, 12(1), 99-108. DOI: 10.1111/j.1654-1103.2001.tb02621.x
[32] Ventura D, Bonifazi A, Gravina MF, Ardizzone GD. Unmanned aerial systems (UASs) for environmental monitoring: A review with applications in coastal habitats. In: Aerial Robots-Aerodynamics, Control and Applications, 2017. DOI: 10.5772/intechopen.69598
[33] Mäyrä J, Tanhuanpää T, Kuzmin A, Heinaro E, Kumpula T, Vihervaara P. Using UAV images and deep learning to enhance the mapping of deadwood in boreal forests. Remote Sensing of Environment, 2025, 329, 114906. DOI: 10.1016/j.rse.2025.114906
[34] Garbarino M, Morresi D, Anselmetto N, Weisberg PJ. Treeline remote sensing: From tracking treeline shifts to multi-dimensional monitoring of ecotonal change. Remote Sensing in Ecology and Conservation, 2023, 9(6), 729-742. DOI: 10.1002/rse2.351
[35] Xie R, Darvishzadeh R, Skidmore AK, van der Meer F, Torres-Rodriguez A, Heurich M. Mapping canopy phenolics in European mixed temperate forests using air- and space-borne imaging spectroscopy. Remote sensing of environment, 2025, 331, 115020. DOI: 10.1016/j.rse.2025.115020
[36] Döweler F, Fransson JES, Bader MKF. Linking high-resolution uav-based remote sensing data to long-term vegetation sampling–A novel workflow to study slow ecotone dynamics. Remote Sensing, 2024, 16(5), 840. DOI: 10.3390/rs16050840
[37] Kesselring J, Humphrey V, Niederberger M, Feigenwinter I, Shekhar A, Buchmann N, et al. Divergence between in situ and satellite-based estimates of forest canopy water content. Remote Sensing of Environment, 2026, 332, 115097. DOI: 10.1016/j.rse.2025.115097
[38] Dainelli R, Toscano P, Di Gennaro SF, Matese A. Recent advances in unmanned aerial vehicle forest remote sensing–A systematic review. Part I: A general framework. Forests, 2021, 12(3), 327. DOI: 10.3390/f12030327
[39] Ma Y, Xie Z, She X, De Boeck HJ, Liu W, Yang C, et al. Combining UAV and sentinel satellite data to delineate ecotones at multiscale. Forests, 2025, 16(3), 422. DOI: 10.3390/f16030422
[40] Wallis CIB, Crofts AL, Jackisch R, Kothari S, Tougas G, Arroyo-Mora JP, et al. Methodological considerations for studying spectral-plant diversity relationships. Remote Sensing of Environment, 2025, 328, 114907. DOI: 10.1016/j.rse.2025.114907
[41] Wei S, Chao Z, Jianyu Y, Honggan W, Minjie C, Anzhi Y, et al. Knowledge-based object oriented land cover classification using SPOT5 imagery in forest-agriculture ecotones. Sensor Letters, 2010, 8(1), 22-31. DOI: 10.1166/sl.2010.1195
[42] Song K, Zhu Z, Qiu S, Olofsson P, Neigh CSR, Ju J, et al. TIF: A time-series-based image fusion algorithm. Remote Sensing of Environment, 2025, 331, 115035. DOI: 10.1016/j.rse.2025.115035
[43] Mishra NB, Mainali KP, Shrestha BB, Radenz J, Karki D. Species-level vegetation mapping in a himalayan treeline ecotone using unmanned aerial system (UAS) imagery. ISPRS International Journal of Geo-Information, 2018, 7(11), 445. DOI: 10.3390/ijgi7110445
[44] Rosas YM, Schmidt IK, Riis-Nielsen T, Vesterdal L, Gundersen P, Byriel DB, et al. Structural diversity, tree species richness and biomass production in new forests on agricultural land. Remote Sensing of Environment, 2025, 330, 114978. DOI: 10.1016/j.rse.2025.114978

[45] Aragoneses E, García M, Tang H, Chuvieco E. A multi-sensor approach allows confident mapping of forest canopy fuel load and canopy bulk density to assess wildfire risk at the European scale. Remote Sensing of Environment, 2025, 318, 114578. DOI: 10.1016/j.rse.2024.114578
[46] Ma Y, Xie Z, She X, De Boeck HJ, Liu W, Yang C, et al. Combining UAV and sentinel satellite data to delineate ecotones at multiscale. Forests, 2025, 16(3), 422. DOI: 10.3390/f16030422
[47] Razzak MA, Awwal MdS, Rahman KMdZ, Bashar K. Diversity and abundance of soil arthropods in Jahangirmagar University campus, Dhaka, Bangladesh. International Journal of Fauna and Biological Studies, 2022, 9(6), 07-12. DOI: 10.22271/23940522.2022.v9.i6a.936
[48] Akmalov S, Atakulov D, Abduraimova D, Ibragimova Z, Ruziyev D, Tadjiboyev S. Green area extraction with using NDVI and ArcGIS pro for Nitra cadastral area. BIO Web of Conferences. EDP Sciences, 2024, 130, 02011. DOI: 10.1051/bioconf/202413002011
[49] Wang R, Wang M, Sun X, Wang J, Li G. Enhancing forest-steppe ecotone mapping accuracy through synthetic apertureradar-optical remote sensing data fusion and object-based analysis. Photogrammetric Engineering & Remote Sensing, 2024, 90(7), 415-426. DOI: 10.14358/PERS.23-00070R2
[50] Hughes D. Hidden in plain sight: Visual knowledge and ecological method. In: Picturing Ecology: Photography and the birth of a new science. Singapore: Springer Nature Singapore, 2022, 271-356. DOI: 10.1007/978-981-19-2515-3_5